# Laboratory Validation of a Compact Single-Scattering Albedo (SSA) Monitor

Julia Perim de Faria[1], Ulrich Bundke[1], *, Andrew Freedman[2], Timothy B. Onasch[2], and Andreas Petzold[1]

[1]Forschungszentrum Jülich GmbH, IEK-8, 52425 Jülich, Germany

[2]Aerodyne Research, Inc., Billerica, MA 01821-3976, USA

*Correspondence to*: Ulrich Bundke (u.bundke@fz-juelich.de)

**Abstract**. An evaluation of the performance and accuracy of a Cavity Attenuated Phase-Shift Single Scattering Albedo Monitor (CAPS $PM_{ssa}$, Aerodyne Res. Inc.) was conducted in an optical closure study with proven technologies: Cavity Attenuated Phase-Shift Particle Extinction Monitor (CAPS $PM_{ex}$, Aerodyne Res. Inc.); 3-wavelengh Integrating Nephelometer (TSI Model 3563); and 3-wavelength filter-based Particle Soot Absorption Photometer (PSAP, Radiance Research). The evaluation was conducted by connecting the instruments to a controlled aerosol generation system and comparing the measured scattering, extinction, and absorption coefficients measured by the CAPS $PM_{ssa}$ with the independent measurements. Three different particle types were used to generate aerosol samples with single-scattering albedos (SSA) ranging from 0.4 to 1.0 at 630 nm wavelength. The CAPS $PM_{ssa}$ measurements compared well with the proven technologies. Extinction measurement comparisons exhibited a slope of the linear regression line for the full data set of 0.96 (-0.02/+0.06), an intercept near zero, and a regression coefficient $R^2$>0.99; whereas, scattering measurements had a slope of 1.01 (-0.07/+0.06), an intercept of less than +/-2×$10^{-6}$ $m^{-1}$ ($Mm^{-1}$), and a coefficient $R^2$~1.0. The derived CAPS $PM_{ssa}$ absorption compared well to the PSAP measurements at low levels (< 70 $Mm^{-1}$) for the small particle sizes and modest (0.4 to 0.6) SSA values tested, with a linear regression slope of 1.0, an intercept of -4 $Mm^{-1}$, and a coefficient $R^2$=0.97. Comparisons at higher particle loadings were compromised by loading effects on the PSAP filters. For the SSA measurements, agreement was highest (regression slopes within 1%) for SSA = 1.0 particles, though the difference between the measured values increased to 9% for extinction coefficients lower than 55 $Mm^{-1}$. SSA measurements for absorbing particles exhibited absolute differences up to 18%, though it is not clear which measurement had the lowest accuracy. For a given particle type, the CAPS $PM_{ssa}$ instrument exhibited the lowest scatter around the average. This study demonstrates that the CAPS $PM_{ssa}$ is a robust and reliable instrument for the direct measurement of the scattering and extinction coefficients and thus SSA. This conclusion also holds as well for the indirect measurement of the absorption coefficient with the constraint that the accuracy of this particular measurement degrades as the SSA and particle size increases.

Keywords: CAPS $PM_{ssa}$, optical closure, single scattering albedo.

## 1 Introduction

Airborne aerosols impact climate directly though the interaction with incident solar light by scattering, generating a cooling effect, or by absorbing it and reemitting infrared radiation, having a heating effect. According to Haywood and Shine (1995), the effect of aerosols on the atmospheric radiation budget in the visible spectral range depends on the aerosols optical depth (AOD), the single-scattering albedo (SSA), and the backscattered fraction (BF). The radiative forcing efficiency (RFE) describes the resulting aerosol direct forcing per unit AOD (Haywood and Shine, 1995;Andrews et al., 2011;Sheridan et al., 2012) and is widely used to describing the radiative impact of a given aerosol type. As an aerosol

intensive parameter the RFE value depends only on SSA and BF. As is stated in the latest IPCC report (Boucher et al., 2013), uncertainties in SSA and the vertical distribution of aerosol contribute significantly to the overall uncertainties in the direct aerosol radiative forcing, while AOD and aerosol size distribution are relatively well constrained.

The measurement of SSA requires the simultaneous but independent observation of two parameters since, by definition, the SSA is the ratio of the scattering to the extinction coefficient (where extinction is the sum of the scattering and absorption – see Equation (1) and (2); the index p refers to the contribution of aerosol particles to overall light extinction, which has also a contribution by gas molecules, identified by the index g not shown in the equation).

$$\sigma_{ep} = \sigma_{ap} + \sigma_{sp} \quad (1)$$

$$SSA = {}^{\sigma_{sp}}/_{\sigma_{ep}} \quad (2)$$

Measuring all three aerosol optical parameters independently allows for the closure of optical properties and thus the determination of uncertainties of the involved instruments.

The aerosol optical parameters are typically measured *in-situ* by instruments such as Integrating Nephelometers (NEPH) for the scattering coefficient (Heintzenberg and Charlson, 1996); photoacoustic (see e.g., Lack et al. (2006); Arnott et al. (2006)) and filter-based methods such as the Particle-Soot Absorption Photometer (PSAP; Bond et al. (1999)), the Multi Angle Absorption Photometer (MAAP; Petzold and Schönlinner (2004)) and more recently the Tricolor Absorption Photometer (TAP/CLAP; Ogren et al. (2017)) for the absorption coefficient; and for the extinction coefficient, the Cavity Ring Down (CRD) technology (Moosmüller et al., 2005) or, since 2007, the Cavity Attenuated Phase Shift Particle Extinction Monitor (CAPS $PM_{ex}$) (Massoli et al., 2010). To measure the SSA using the optical closure approach involves separate instruments with different principles and uncertainties, leading to potential sources of significant errors and biases.

A novel instrument based on cavity attenuated phase-shift technology and incorporating an integrating sphere was recently developed by Aerodyne Research, Inc. This novel instrument represents a major step forward in the observation of aerosol optical properties since it simultaneously measures two of the three aerosol optical parameters from the same air sample, reducing the potential sources of sampling biases (Onasch et al., 2015). The two main applications of the CAPS $PM_{ssa}$ instrument, apart from the direct measurement of scattering and extinction coefficients, are the indirect measurement of the aerosol absorption coefficient and the measurement of the single-scattering albedo. A few recent *in-situ* application studies of the CAPS $PM_{ssa}$ instrument are already available (Han et al., 2017;Corbin et al., 2018). The present optical closure study intends to quantify uncertainties in the measurement of the primary aerosol optical properties and the resulting SSA by the CAPS $PM_{ssa}$ for several types of laboratory aerosol by applying a full set of established instrumentation for measuring the extinction (CAPS $PM_{ex}$), absorption (PSAP), and scattering (Integrating Nephelometer TSI Model 3563) coefficients at multiple wavelengths.

## 2 Instruments and Methods

### 2.1 Instrumental Set-up

The laboratory study was conceived to evaluate the operational principle of the CAPS $PM_{ssa}$ and its performance and accuracy when compared to proven technologies. The instrumental set-up used is shown in Figure 1.

In this study, similar to previous work (Massoli et al., 2010;Petzold et al., 2013); two collision-type aerosol generators (TSI Model 3076) were used; one containing a solution of deionized water and purely scattering aerosol, Ammonium Sulphate (AS), and a second containing absorbing aerosol, water-soluble colloidal graphite (Aquadag – AD – from Agar Scientific) or Black Carbon (REGAL 400R Pigment Black – BC – from Cabot Corporation). The SSA of the

dispersed aerosol ranged from approximately 0.4 (pure AD or BC) to 1.0 (pure AS), with the modal value of the particle size distribution being below 100 nm in all cases. A drying tube filled with silica gel was positioned after each particle generator in order to reduce the relative humidity below 30%. Once the samples were passed through the dryer, they entered a mixing chamber where effective ensemble particle SSA values of 0.4 < SSA < 1.0 could be produced by mixing aerosol flows containing both absorbing and scattering aerosols. The aerosol generation set-up specifications are shown in Table 1, whereas Table 2 compiles the information about the applied instrument and correction schemes. The SSA of the mixture containing AS and AD, was controlled by the online measured SSA measured by the CAPS $PM_{ssa}$.

Three mass flow controllers (MFC), one at each generator's head and a third after the mixing chamber, supplied particle-free compressed air to the sample to both reach the desired humidity and particle number concentration and to make-up the flow required by the instruments. The particle number concentration was measured by a condensation particle counter (CPC).

**Table 1. Type of generated aerosol, targeted SSA (630 nm), and targeted max. aerosol extinction values**

| Aerosol type | Estimated /Expected SSA | Run 1 200 $Mm^{-1}$ | Run 2 150 $Mm^{-1}$ | Run 3 100 $Mm^{-1}$ | Run 4 50 $Mm^{-1}$ | Run 5 25 $Mm^{-1}$ |
|---|---|---|---|---|---|---|
| Aquadag (AD) | 0.4 | x | x | x | x | x |
| Black Carbon (BC) | 0.4 | | x | x | x | x |
| Mixture (AS+AD) | 0.6 | | | x | x | x |
| Ammonium Sulphate (AS) | 1.0 | | x | x | x | x |

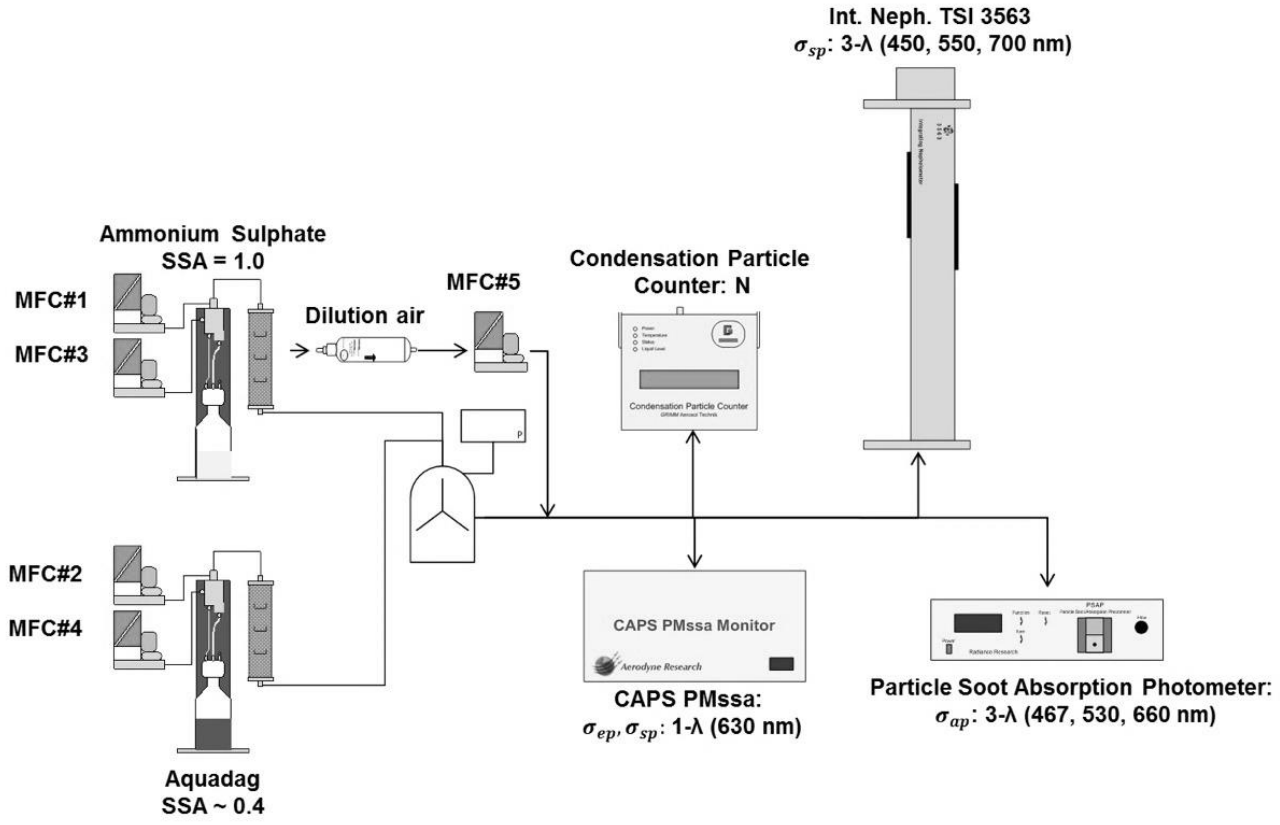


**Figure 1. Instrumental set-up applied in the optical closure study**

**Table 2. List and specifications of optical instrumentation and applied correction algorithms**

| Instrument | Manufacturer | Property | λ (nm) | Aerosol | Correction Algorithm |
|---|---|---|---|---|---|
| CAPS $PM_{ssa}$ | Aerodyne Research Inc. | $\sigma_{sp}$, $\sigma_{ep}$ | 630 | AS, AD, BC, MIX | Mie Amigo (Aerodyne) for $\sigma_{sp}$ truncation correction (Onasch et al., 2015) |
| CAPS $PM_{ex}$ | Aerodyne Research Inc. | $\sigma_{ep}$ | 630 | AS, AD, BC, MIX | No correction required |
| NEPH | TSI Inc. | $\sigma_{sp}$ | 450, 550, 700 | AS | Müller et al. (2009), Anderson et al. (1998) |
| | | | | AD, BC, MIX | Massoli et al. (2009) |
| PSAP | Radiance Research Inc. | $\sigma_{ap}$ | 467, 530, 660 | AS, AD, BC, MIX | Ogren (2010) and Virkkula (2010) |

The samples were produced at up to five nominal concentration levels, as shown in Table 1, defined by the aerosol extinction. This was achieved by holding the aerosol generation system constant (MFC#3 and MFC#4) and regulating the make-up air MFCs (MFC#1, MFC#2 and MFC#5). Extinction coefficient levels were varied from ~10 up to 200 $Mm^{-1}$. For each level, a sampling time of at least 5 minutes was sustained.

To ensure an isoaxial, isokinetic sampling by all instruments, special sampling tips made of stainless steel were designed such that the sample air extraction tips were each concentrically placed along the centre line of the sample tube of 1 inch inner diameter. The inlet nozzles diameters are dimensioned such that the flow velocities in the sample tube and inside extraction tip nozzles match. Distances between the extraction points for the different instruments were 20 cm.

The nephelometer was calibrated using $CO_2$ (high span gas) and particle-free air (low span gas), before starting the experiments. The calibration procedure includes also, as recommended by the manufacturers, the calibration of scattering channel of the CAPS $PM_{ssa}$, against the extinction channel of the instrument. For the filter-based absorption instruments, no calibration is necessary since they both operate with a blank filter in parallel as reference (see description in the subsections below).

The optical instruments were placed downstream of the generation system, measuring simultaneously, as shown, and will be described in more detail in the following subsections.

### 2.1.1 Integrating Nephelometer

In this optical closure study, an integrating nephelometer (NEPH) of the type TSI Model 3563 was used. The NEPH collects scattering measurements both in the forward and backscatter directions at three wavelengths 450, 550, and 700 nm (Heintzenberg et al., 2006).

The NEPH data was corrected for truncation angle effects using the approach proposed by Massoli et al. (2009) for strongly light-absorbing aerosols (equations 3 and 4 and Table 3). For predominantly light-scattering aerosols, the approaches proposed by Anderson et al. (1996) and Müller et al. (2009) were used (equation 5 and Table 4).

$$C = MAX\{1.0, v_0 + v_1 \exp(v_2 * (3.25 - å)) + C(n)\} \quad (3)$$

where å is the Ångstrom exponent (equation 7), $C'(n)$ is an optional correction for submicron distributions. $C(n)$ is equal to 0 for å ≥2.8, and to

$$C(n) = v_3(2.8 - å) * (\frac{1}{(n-1)} - \frac{1}{0.48}) \quad (4)$$

and $v_0, v_1, v_2 \; and \; v_3$ are given in Tab and n is the real part of the refractive indices.

120

**Table 3. Coefficient values for $v_0, v_1, v_2$ and $v_3$ for equations 3 and 4 (Massoli et al., 2009).**

| | $v_0$ | $v_1$ | $v_2$ | $v_3$ |
|---|---|---|---|---|
| 698 nm sub-µm | 0.8627 | 0.1423 | 0.1816 | 0.0306 |
| 554 nm sub-µm | 0.8511 | 0.1589 | 0.2153 | 0.0439 |
| 453 nm sub-µm | 0.8863 | 0.1327 | 0.2758 | 0.0610 |
| 698 nm all | 0.9869 | 0.0182 | 0.7980 | |
| 554 nm all | 0.9948 | 0.0152 | 0.8951 | |
| 453 nm all | 1.0072 | 0.0118 | 1.0036 | |

$$C = a + b * å \tag{5}$$

125 **Table 4. Values for a and b for equation 5 for Anderson and Ogren (1998) and Müller et al. (2011).**

| | | Blue (450 nm) | | Green (550 nm) | | Red (700 nm) | |
|---|---|---|---|---|---|---|---|
| **Ångstrom exponent** | | å(B/G) | | Å(B/R) | | Å(G/R) | |
| | | a | b | a | b | a | b |
| Anderson et al. (1998) | No cut | 1.365 | -0.156 | 1.337 | -0.138 | 1.297 | -0.113 |
| | Sub-µm | 1.165 | -0.046 | 1.152 | -0.044 | 1.120 | -0.035 |
| Müller et al. (2011) | No cut | 1.345 | -0.146 | 1.319 | -0.129 | 1.279 | -0.105 |
| | Sub-µm | 1.148 | -0.041 | 1-137 | -0.040 | 1.109 | -0.033 |

### 2.1.2 Particle-Soot Absorption Photometer

The PSAP is a filter-based three wavelength (467, 530, 660 nm) instrument, manufactured by Radiance Research, that provides continuous measurement of the light absorption coefficient. The instrument uses two spots on a quartz fibre filter; one receives the particle containing sample, and the second clean air. The instrument measures the difference in the
130 transmission of light between a loaded and a blank filter spot (Bond et al., 1999). Two absorption coefficient data correction were used and evaluated: Ogren (2010) and Virkkula (2010). The best fitting corrections is the one shown in each result subsection.

In his approach, Ogren (2010) furthers the corrections from Bond et al. (1999), considering the filter area correction and wavelength adjustment, as shown in equation 6, for the complete absorption coefficient measurement.

135
$$\sigma_{ap} = 0.85 \left(\frac{Q_{PSAP}}{Q_{meas}}\right)\left(\frac{A_{meas}}{A_{PSAP}}\right)\frac{\sigma PSAP[\lambda]}{K_2} - \frac{K_1}{K_2}\sigma_{sp}[\lambda] \tag{6}$$

where $\sigma_{ap}$ is the absorption coefficient of the desired wavelength, $Q_{PSAP}$ is the flow recorded by the instrument, $Q_{meas}$ is the measured flow, $A_{meas}$ is the real area of the filter, $A_{PSAP}$ is the manufacturer supplied area of the filter, $\sigma_{PSAP}$ is the measured absorption coefficient at a certain wavelength ($\lambda$), $K_1$ and $K_2$ are constants given ($0.02 \pm 0.02$ and $1.22 \pm 0.20$, respectively) and $\sigma_{sp}$ is the scattering coefficient measured at the same wavelength as $\sigma_{PSAP}$.

140 Virkkula (2010) derives a new correction from a field campaign, including as a function factor the single scattering albedo, as shown in equation 7.

$$\sigma_{ap} = (k_0 + k_1(h_0 + h_1\omega_0)\ln(Tr))\sigma PSAP[\lambda] - s\sigma_{sp}[\lambda] \quad (7)$$

where $\sigma_{ap}$ is the absorption coefficient of the desired wavelength, $k_0$, $k_1$, $h_0$, $h_1$ and s are constants given (Table 5), $\omega_0$ is the single scattering albedo, Tr is the measured transmission, $\sigma_{PSAP}$ is the value measured by the PSAP and $\sigma_{sp}$ is the scattering coefficient measured at the same wavelength as $\sigma_{PSAP}$.

**Table 5. Constant values given by Virkkula (2010) for equation 7**

| Constant | 467 nm | 530 nm | 660 nm |
|---|---|---|---|
| $k_0$ | 0.377 ± 0.013 | 0.358 ± 0.011 | 0.352 ± 0.013 |
| $k_1$ | -0.640 ± 0.007 | -0.640 ± 0.007 | -0.674 ± 0.006 |
| $h_0$ | 1.16 ± 0.05 | 1.17 ± 0.03 | 1.14 ± 0.11 |
| $h_1$ | -0.63 ± 0.09 | -0.71 ± 0.05 | -0.72 ± 0.16 |
| s | 0.015(0.009, 0.020) | 0.017(0.012, 0.023) | 0.022(0.016,0.028) |

### 2.1.3 The CAPS $PM_{ex}$

The CAPS $PM_{ex}$ system, described in detail and assessed in several studies, such as Massoli et al. (2010), Petzold et al. (2013) and Perim de Faria et al. (2017) measures light extinction by determining the change in signal phase shift caused by the introduction of particles into an optical cavity. The use of high reflectivity mirrors (reflectivity approx. 99.99%) in the optical cavity creates the long measurement path of approx. 2 km required to measure very low values of light extinction (LOD of 1-2 $Mm^{-1}$ in 1 second sample period).

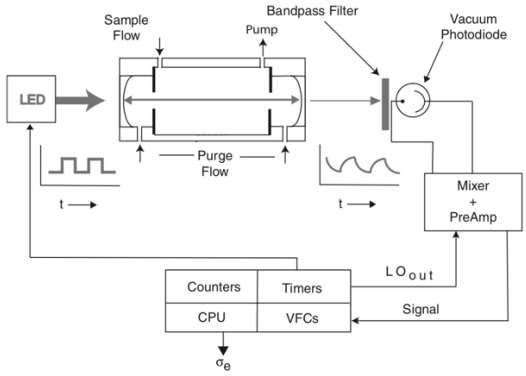


**Figure 2. Overview of the main components and operation principle of the CAPS $PM_{ex}$ instrument (Massoli et al., 2010)**

### 2.1.4 The CAPS $PM_{ssa}$

The CAPS $PM_{ssa}$ (Onasch et al., 2015), uses the same principle to measure light extinction as the CAPS $PM_{ex}$, but it also contains, located at the centre of the measurement cell, a 10 cm diameter integrating sphere capable of measuring light scattering on the same aerosol sample, as shown in Figure 3. The integrating sphere acts as an integrating nephelometer, which measures the scattering of light by particles at all angles, only excluding the near 0 and near 180° angles since the opening of the extinction chamber is located in these directions, allowing the sample and light beam to pass through. The sphere shows 98-99% Lambertian reflectance efficiency due to its high reflectivity coating (Avian D from Avian Technologies). The usage of an integrating sphere increases the collection of scattered light at the photomultiplier compared to a traditional cosine corrected detector arrangement.

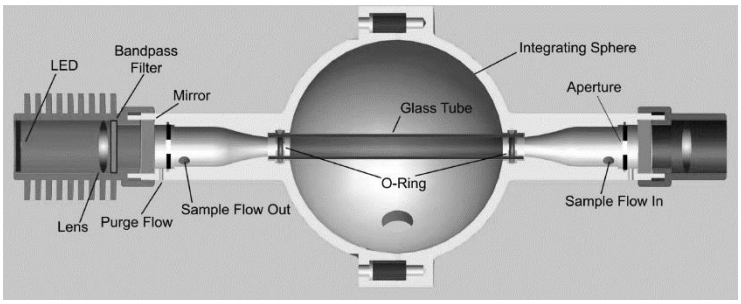


**Figure 3. CAPS PMssa components and set-up (Onasch et al., 2015).**

The scattering channel is calibrated against the extinction channel using either small particles (<250 nm) that have SSA=1.0 or $CO_2$ (as done in this study, shown in Figure 4 – slope, offset and $R^2$ calculated using the 1-second resolution data; the scatter plot shows the average and standard deviation) and set equal to the extinction measurement. Thus, the monitor should be thought of as providing separate extinction and SSA values with the scattering channel a derived measurement. This calibration procedure also allows the user to prove monitor linearity over a wide range of optical extinctions without the limitation of using individual gases with sometimes not particularly well-known Rayleigh scattering coefficients.

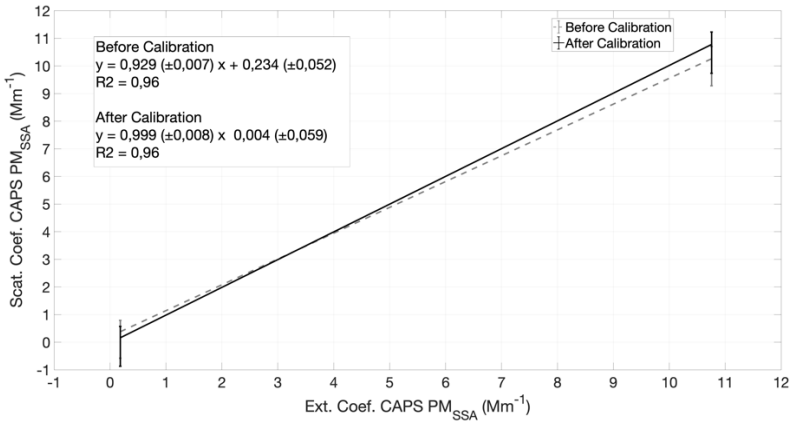


**Figure 4. Scatterplot of the correlation of the extinction and scattering channel of the CAPS $PM_{ssa}$ before and after the calibration using $CO^2$.**

The sample flow in the instrument is set to 0.85 lpm and is controlled by a critical orifice. The measurement sample enters the chamber in one end and exits through an opening located in the other end flowing through a glass tube inside the integrating sphere (Figure 3). The mirrors are kept particle-free by a continuously flowing purge flow (25 $cm^3$ $min^{-1}$). Petzold at al. (2013) showed that this purge flow shortens the measurement path and dilutes the sample and requires a correction factor. As done for the CAPS $PM_{ex}$, a new correction factor was developed, by using monodisperse polystyrene spheres (PSL) of know size, for the CAPS $PM_{ssa}$. Due to the cell geometry, the new correction factor was slightly larger than the one found for the extinction monitor, 1.37 and 1.27, respectively (Onasch et al., 2015). The noise of the instrument, trunction angle and instrument uncertainty have also been studied by Onasch et al. (2015). The values found were all below 1 $Mm^{-1}$ for the noise levels (1σ, 1s) for all wavelengths. For the case of this particular instrument (630 nm), the truncation correction was determined below 4% for typical ambient conditions. The uncertainty was estimated at ±0.03 for SSA equal to 1 (PSL and ammonium sulphate) and decreases to ±0.01 as the SSA goes down.

The baseline determination system is identical to the one used in the CAPS $PM_{ex}$, in which filtered and thus particle-free sample air fills the measurement chamber and is used to quantify contributions of gas molecules to the

instrument response by Rayleigh scattering and potential absorption of light, and to determine interferences of system components. Both the CAPS $PM_{ex}$ and CAPS $PM_{ssa}$ used in this study operate at a wavelength of 630 nm and thus show minimal interference from absorption by ambient gaseous species like $NO_2$ and $H_2O$.

## 2.2 Data Treatment

All multi-wavelength instruments were adjusted to match the other instruments' wavelengths for the intercomparison by using the Ångström exponent approach; see Equation (8) and (9),

$$å = -\left. log\frac{\sigma_x}{\sigma_y} \right/ log\frac{x}{y} \quad (8)$$

$$\sigma_w = \sigma_y \times (w/y)^{-å} \quad (9)$$

where å is the Ångström exponent, σ is the optical property measured (extinction, scattering or absorption coefficient), x and y are the operating wavelengths of the instrument, and w refers to the wavelength, to which the property should be adjusted. For a better understanding of the wavelength adjustment, the complete description is given in Figure 3 from Petzold et al. (2013).

All instruments provide 1 second resolution data. Data was collected over 5 minutes for each experimental point to remove any effect of differences in response times and fluctuations in the aerosol generation system. The data was averaged for each extinction/scattering/absorption level, and the standard deviation was calculated from the mean.

Standard linear regression analysis was performed for the mean values of each level. For the cases with the standard deviation of the intercept value being higher than the value itself, the regression model interception was forced to zero intercept, since the intercept value shows no significant difference to zero.

## 2.3 Measurement uncertainties

This paper does not address in any explicit way, nor was it designed to address, the question of the absolute uncertainties of the different measurement techniques. It was designed to address the question of how well they correlate. Thus, the results are given in correlation coefficients (slope and intercept) and their statistical uncertainties.

For this reason, this section compiles the reported absolute errors by the relevant instrument papers.

**Table 6 Measurement uncertainties for the different instruments as reported by the relevant instrument papers.**

| Instrument | sep | ssp | sap | SSA | Reference | Comments |
|---|---|---|---|---|---|---|
| CAPS PMssa | 5% | 8% | 13% (SSA=0.5) and 5%(SSA=1.0) | 3% | (Onasch et al., 2015) | Estimates for polydispers aerosol. Absorption uncertainty is dependent upon the SSA value |
| NEPH | | <10% | | | (Anderson et al., 1996)& (Massoli et al., 2010) | for sub micrometer particles |
| CLAP | | | 8% | | (Ogren et al., 2017) | |
| PSAP | | | 8% | | (Muller et al., 2014) | |
| NEPH+PSAP | 7% | | | | (Petzold et al., 2013) | (3-sigam) obtained for the test aerosol inversion of NEPH+PSAP data |

## 3 Results and Discussion

In this section, we present the results and relevant discussion of findings for the optical closure study. All the measurements presented here were corrected to the CAPS $PM_{ssa}$ operational wavelength of 630 nm.

### 3.1 Extinction Coefficient

The extinction coefficient measured by the CAPS $PM_{ssa}$ was analysed in comparison with proven technologies. On the direct measurement of $\sigma_{ep}$, we compared the two CAPS systems for AS and AD (Petzold et al., 2013). The direct measurement of $\sigma_{ep}$ from the CAPS $PM_{ssa}$ was also compared with the indirect measurement given by the sum of the absorption coefficient measured by the PSAP with the scattering coefficient measured by the NEPH for BC, AD, and MIX (as defined in Table 1) – shown as PSAP+NEPH. For AS with the measured SSA value of 1.0, extinction coefficients provided by the CAPS extinction channels and scattering coefficients provided by the CAPS scattering channel and the NEPH instrument are used for the evaluation of the light scattering measurements in the next subsection. The time series for the extinction channels are shown in Figure 5 and the averages and standard deviations for each test point are shown in Table A1 in the supplemental information. The higher variability observed in the last plot of the figure is due to particle load fluctuations from generation system when operating at very high loads.

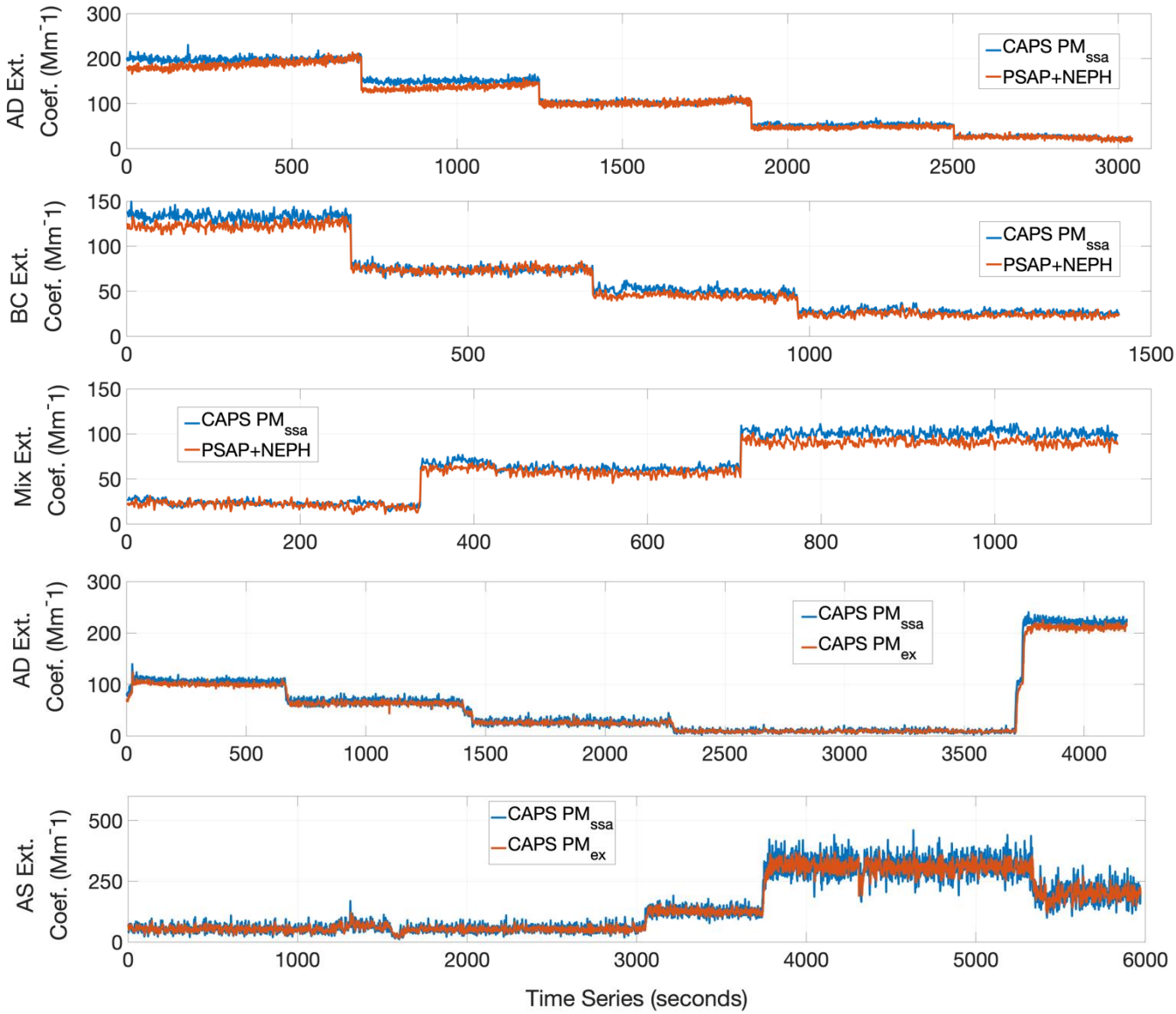


**Figure 5. Time series of the parallel measured extinction coefficients by the different instruments. Instruments used : CAPS $PM_{ex}$, CAPS $PM_{SSA}$ and the sum of absorption- and scattering coefficients measured by PSAP and NEPH as noted in the legend for the individual subplots. The test aerosolsused are noted in the caption of the y-axis of the individual subplots.**

Figure 6 shows the scatter plot of the measured extinction coefficient for the two CAPS systems for AD and AS and the comparison with the sum of the NEPH and PSAP for AD and BC. The best results for the AD and BC were found when applying the Massoli et al. (2009) correction with the assumption, that no particle size cut has been used for the inlet system (no-cut approach) to the NEPH data, and Virkkula (2010) for strongly light-absorbing aerosols AD and BC to the PSAP data. For the mixture, the applied corrections were Anderson et al. (1998) for the NEPH data and Ogren (2010) for the PSAP data. The extinction channels from the two CAPS and the sum of the NEPH and PSAP (PSAP-NEPH) signals show a good agreement for all aerosol types, with linear regression slopes (m) between 0.94 and 1.02 and correlation coefficients above 0.99 (all regression analysis data for the averaged values of each level is presented in Table 7 together with their standard deviation). For the linear regression analysis of the full data set including all types of aerosols, the slope found was 0.96 ($R^2$=0.99) for the comparison of the CAPS $PM_{ssa}$ extinction data with the sum of NEPH and PSAP data, and 0.97 ($R^2$=1.00) for the comparison of the CAPS $PM_{ssa}$ and CAPS $PM_{ex}$ extinction data. The slopes of the regression

analysis and their standard deviation are shown in Figure 7 as a function of the sampled aerosol single-scattering albedo. As it can be seen there is no systematic difference in the slope with increase or decrease of the aerosol SSA.

**Table 7 Linear regression parameters including the slope (M), standard deviation of the slope (Std m), intercept (B), standard deviation of intercept (std b), and linear regression coefficient ($R^2$) for the comparison of the CAPS $PM_{ssa}$ extinction channel with proven technologies**

| Aerosol | Reference Instrument | Estimated SSA | M | Std m | B | Std b | $R^2$ |
|---|---|---|---|---|---|---|---|
| AD | PSAP+NEPH | 0.4 | 0.94 | 0.01 | 0.00 | < 0.01 | 1.00 |
| BC | PSAP+NEPH | 0.4 | 1.00 | 0.01 | 0.00 | < 0.01 | 1.00 |
| MIX | PSAP+NEPH | 0.6 | 1.02 | 0.00 | 0.00 | < 0.01 | 1.00 |
| ALL | PSAP+NEPH | NA | 0.95 | 0.01 | 0.00 | < 0.01 | 0.99 |
| AD | CAPS $PM_{ex}$ | 0.4 | 0.95 | 0.00 | 0.00 | < 0.01 | 1.00 |
| AS | CAPS $PM_{ex}$ | 1.0 | 1.00 | 0.00 | 0.00 | < 0.01 | 1.00 |
| ALL | CAPS $PM_{ex}$ | NA | 0.97 | 0.00 | 0.00 | < 0.01 | 1.00 |

It is worth noting that for the particular instruments used in our study, the standard deviation for the extinction data of the CAPS $PM_{ssa}$ is larger than for the extinction data provided by the CAPS $PM_{ex}$ (horizontal error bars). This finding is shown in the histogram of the extinction channel from one measurement level (in this case the used dataset refers to the 25 $Mm^{-1}$ target-level for AD aerosol) for both equipment (Figure 8). Thus, the precision of this particular CAPS $PM_{ssa}$ is lower than the precision of the CAPS $PM_{ex}$. Regarding the precision of the CAPS $PM_{ssa}$ in comparison with proven technologies, the standard deviation found in this study for both cases are comparable. The precision in the CAPS $PM_{ex}$ and PSAP+NEPH extinction measurements found in this study are very similar to the one found by Petzold et al. (2013), in which an excellent correlation (slope of 0.99) was found for the laboratory comparison between the same instruments using highly absorbing aerosol, exclusive scattering aerosol and mixtures of both.

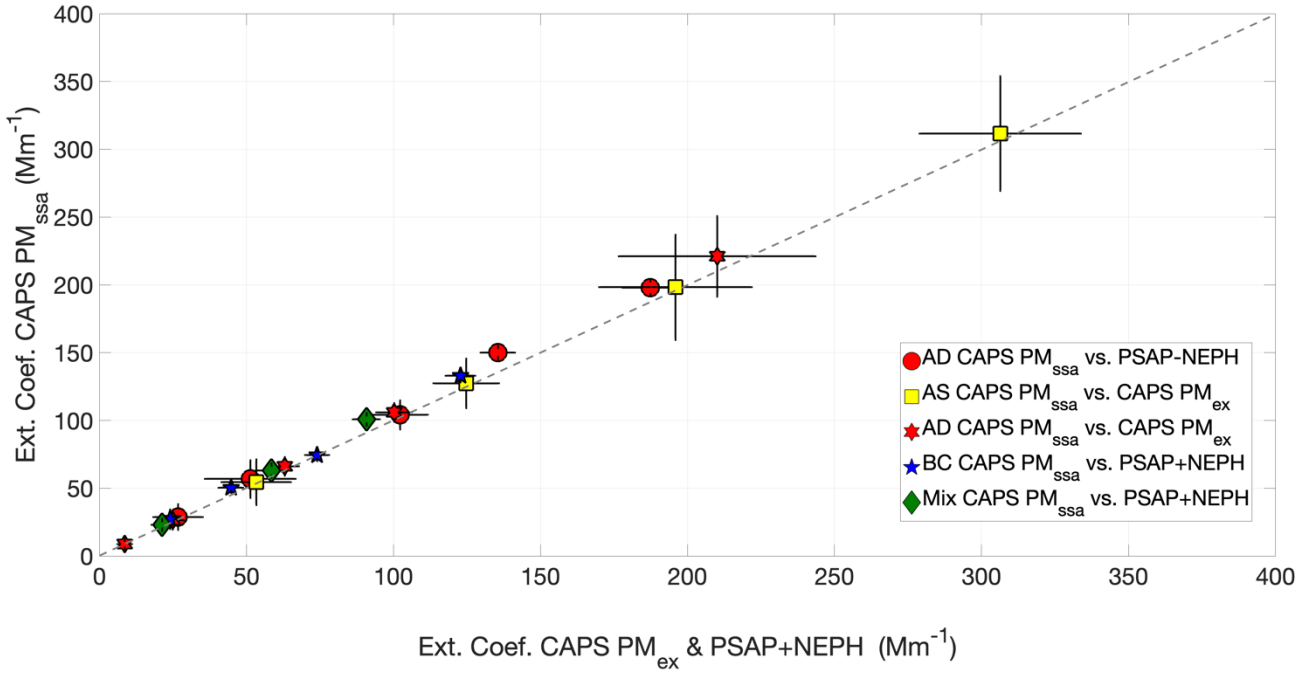


**Figure 6. Comparison result of the extinction channel of the CAPS PM$_{ssa}$ with the CAPS PM$_{ex}$ and the combination PSAP+NEPH for for the different aerosol types (dashed line is the identity line (i.e., 1:1 line)).**

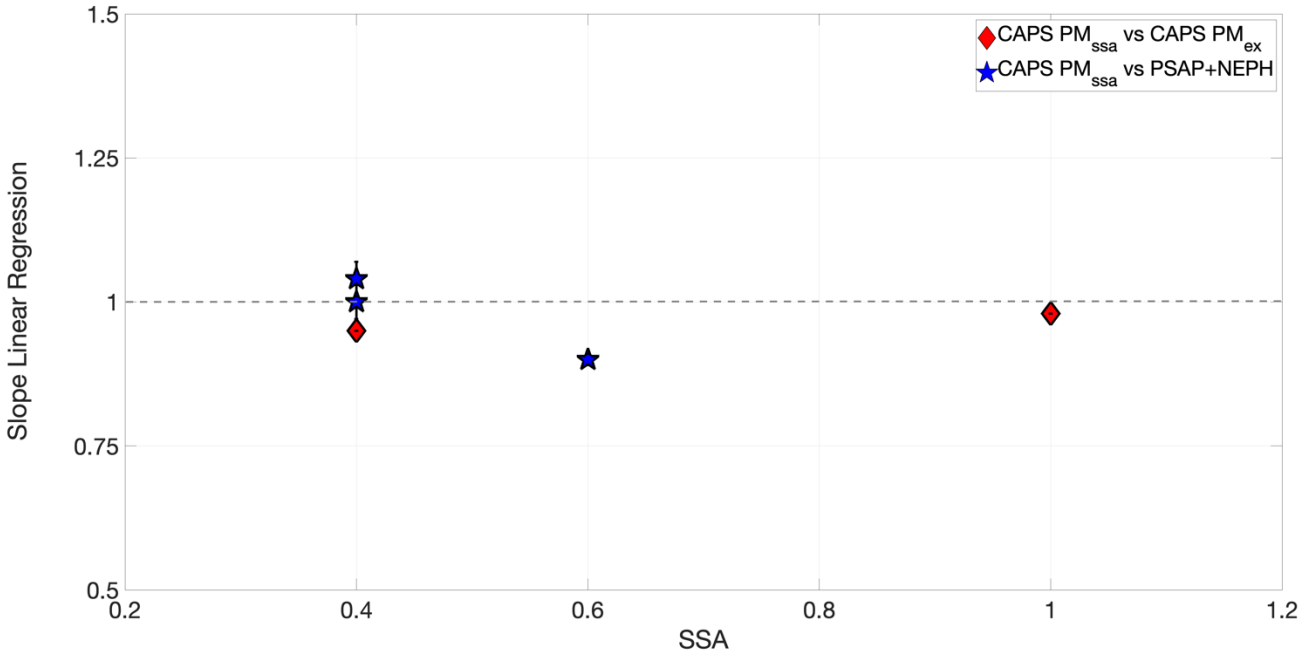


**Figure 7. Slope values of the linear regressions of measured particle extinction as a function of nominal aerosol SSA for the different instrument intercomparison.**

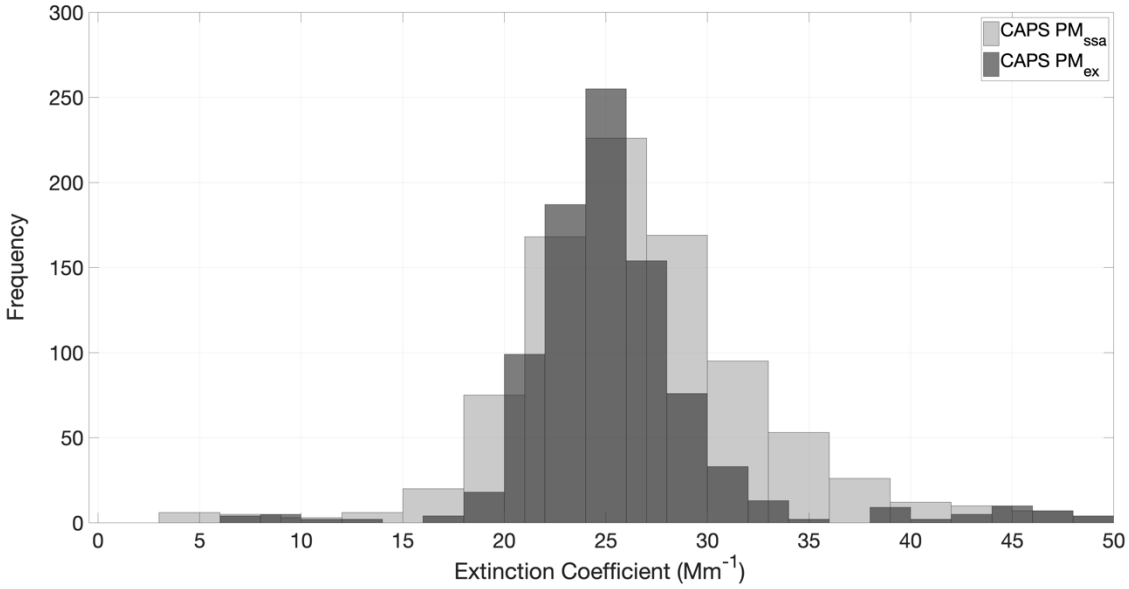


**Figure 8. Frequency of extinction coefficient measurement for the CAPS $PM_{ssa}$ and $PM_{ex}$ systems at the nominal 25 $Mm^{-1}$ (level 5) test point for AD.**

### 3.2 Scattering Coefficient

The scattering channel of the CAPS $PM_{ssa}$ was evaluated in comparison to the NEPH measurements for AD, BC, AS, and MIX (Table 1). The time series of scattering coefficient data for the various aerosol runs is shown in Figure 9. Supplemental Table A2 shows the average and 1-σ standard deviation obtained for the targeted scattering coefficient levels. Within the error bars of the two instruments we could not observe a systematic deviation of both either in the average or in the standard deviation of the measured values. The precision of both instruments for the measurement of scattering coefficient is very similar.

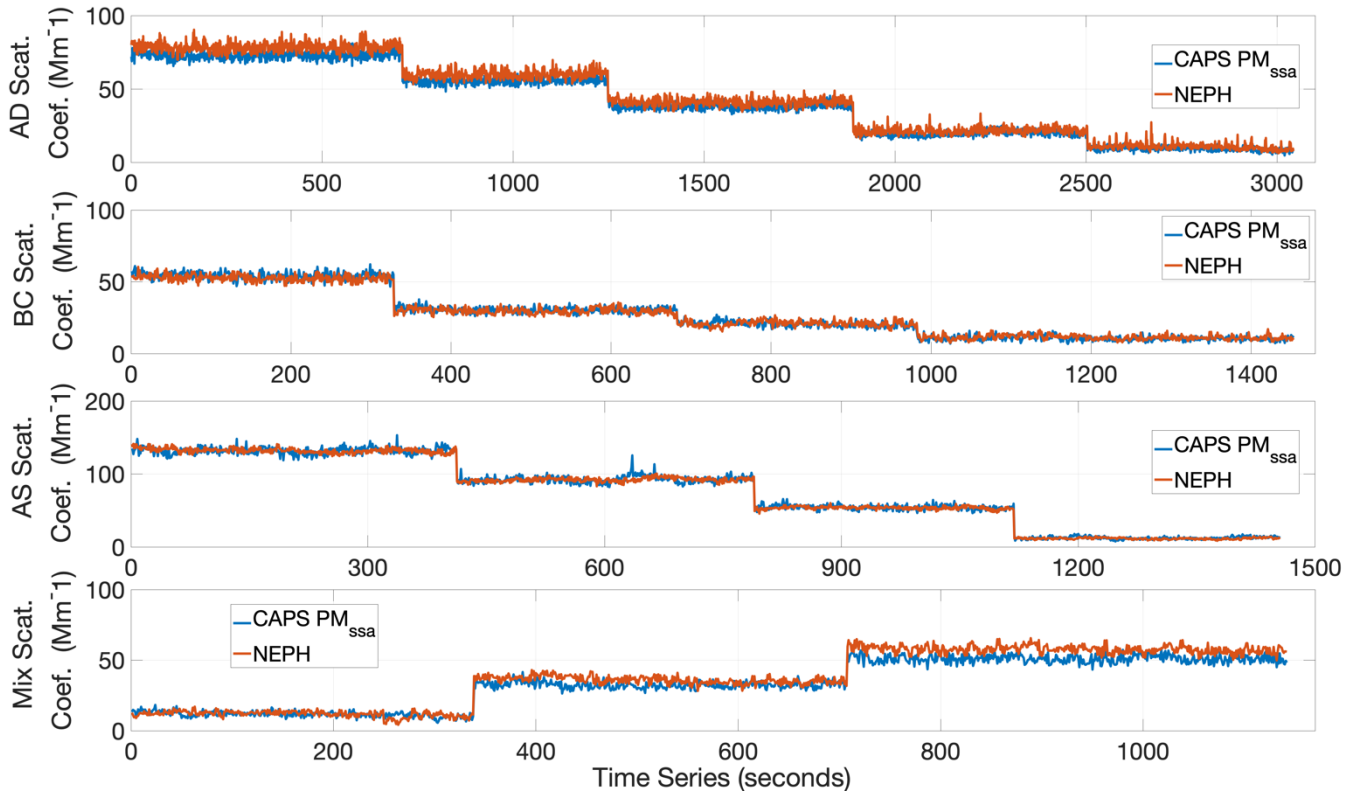


**Figure 9. Time series of the scattering coefficients parallel measured by the different instruments: CAPS $PM_{SSA}$ and NEPH for the different aerosol types (BC (top-) AS(middle-) and Mix (bottom-figure).**

Figure 10 shows the scatter plot of the 1-second average and standard deviation of the CAPS $PM_{ssa}$ against NEPH. As it can be seen from Figure 10 and the data compiled in Table 8, the agreement with the NEPH measurements is excellent, with less than 8% difference in the slope, offset smaller than 2.00 $Mm^{-1}$ and correlation coefficient of 1.00 for all aerosol types. The slope value and standard deviation as a function of SSA is shown in Figure **11**. For the AD, BC and Mix cases, the NEPH data was corrected with the Massoli et al. (2009) approach. For the AS case both the Anderson et al. (1998) and Müller et al. (2011) were applied and the results given were practically the same, less than 2% in the slope and less than 1.00 $Mm^{-1}$ difference in the offset. For the overall measurement linear regression model, including all types of aerosols, the slope found was 1.01 ($R^2$=1.00) for the comparison of the CAPS $PM_{ssa}$ with the NEPH.

**Table 8. Linear regression parameters including the slope (M), standard deviation of the slope (Std m), intercept (B), standard deviation of intercept (std b), and linear regression coefficient ($R^2$) for the comparison of the CAPS $PM_{ssa}$ scattering channel with NEPH**

| Aerosol | Reference Instrument | SSA | m | Std m | b | Std b | $R^2$ |
|---|---|---|---|---|---|---|---|
| AS | NEPH | 1.00 | 1.02 | 0.00 | -0.72 | 0.14 | 1.00 |
| AD | NEPH | 0.40 | 0.98 | 0.00 | 1.48 | 0.18 | 1.00 |
| BC | NEPH | 0.40 | 0.94 | 0.01 | 1.22 | 0.28 | 1.00 |
| MIX | NEPH | 0.60 | 1.07 | 0.01 | -0.55 | 0.50 | 1.00 |
| ALL | NEPH | NA | 1.01 | 0.01 | 0.00 | 0.00 | 1.00 |

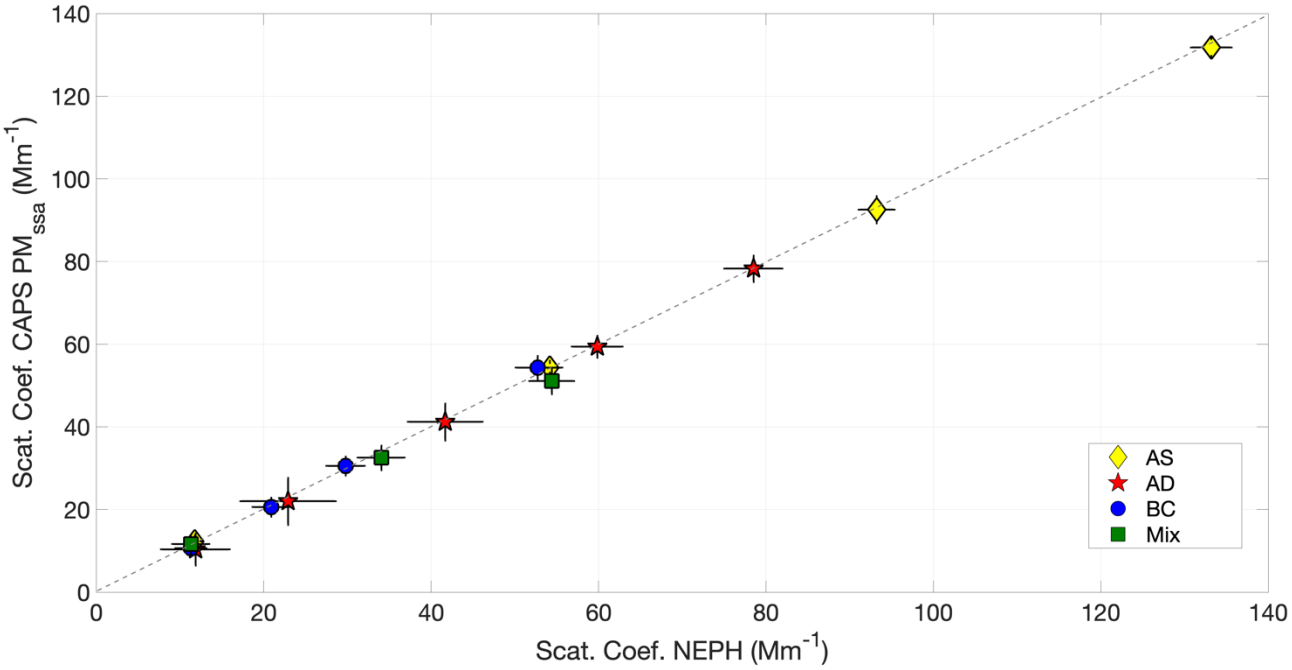


**Figure 10. Comparison result of the scattering channel of the CAPS PM$_{ssa}$ with the measurements from the NEPH for the different aerosol types (**dashed line is the identity line (i.e., 1:1 line)**).**

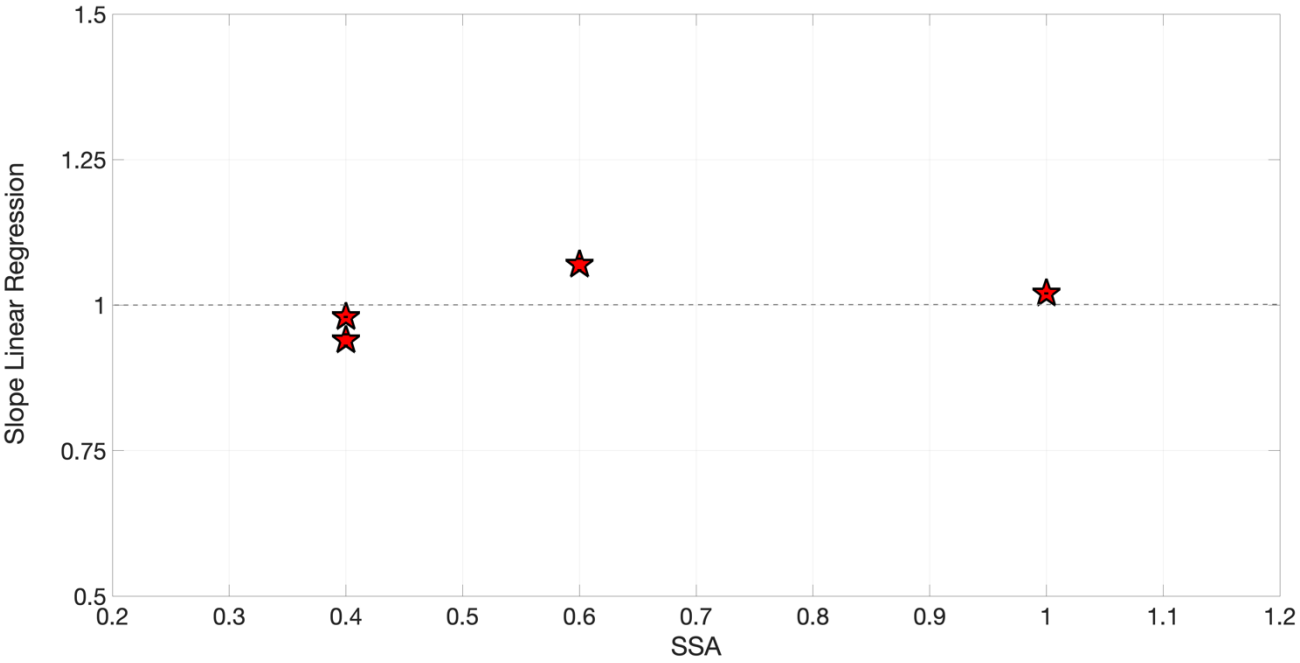


**Figure 11. Slope values of the linear regression as a function of expected aerosol SSA for CAPS PM$_{ssa}$ and NEPH; uncertainty of the slopes is below the resolution of the symbols; see Table 8.**

### 3.3 Absorption Coefficient

In spite of the fact that the CAPS PM$_{ssa}$ is not capable of directly measuring the absorption coefficient, the values can be derived as the difference of the extinction and the scattering coefficients; see Equation (1). From the difference of the two CAPS PM$_{ssa}$ channels the calculated absorption coefficients were compared to the direct measurement by the PSAP. In this

analysis, when operating with a mixture of AS and AD, the PSAP data were treated using the correction from Ogren (2010). The time series for the measurement of the different aerosols are shown in Figure 12 whereas Supplemental Table A3 shows the average and 1-σ standard deviation obtained for the targeted absorption coefficient levels.

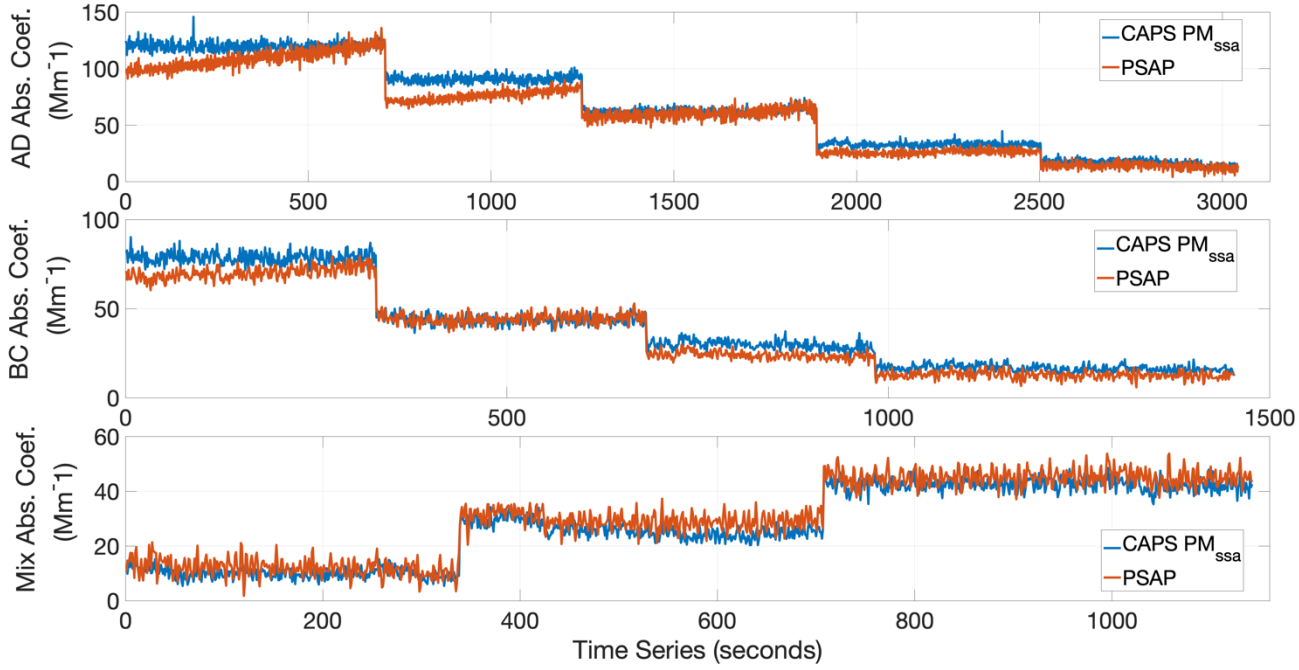


**Figure 12. Time series (in seconds) of the parallel measurements of the absorption coefficient for the different test aerosols (TOP (Aquadag AD, Middle BC, Butttom (Mix) by the PSAP and the CAPS $PM_{SSA}$ (as a result of the substraction of the scattering coefficient from the extinction coefficient).**

The scatter plot for the average measured values from both methods for all levels is shown in Figure 13, whereas the results of the linear regression analysis are compiled in Table 9. The agreement between the methods is good, with deviations below 11% in the slope, and offsets less than 2.0 $Mm^{-1}$. The correlation coefficient is above 0.98 for all cases. For the full data set of CAPS $PM_{ssa}$ and PSAP absorption coefficient data including all types of aerosols, the slope is 0.91 with a correlation coefficient of $R^2$=0.98. Figure 13 demonstrates that for higher absorption coefficients, the two methods deviate more strongly than for lower absorption coefficients. This is mainly caused by the correction algorithm applied to the PSAP data (also seen on Figure 12); filter loading corrections are significantly larger for higher absorption coefficient levels than for lower absorption coefficient levels. If the three data points for higher absorption coefficient data ($\sigma_{ap}$ > 70 $Mm^{-1}$) are removed from the regression analysis, the slope value increases to 1.00 ($R^2$=0.97), although with an offset of -3.64. The increase in the absorption coefficient observed in Figure 12 for the higher levels of AD and BC, is related to the transmission decay of the filter in the PSAP and the correction algorithm chosen for this study. This finding proves that, although the CAPS $PM_{ssa}$ cannot directly measure aerosol light absorption, it provides a rather reliable measurement of the absorption coefficient of the sampled aerosol, at least for the small particle sizes and intermediate SSA values sampled in this study. The accuracy of absorption measurements by the two channels of the CAPS $PM_{ssa}$ may be significantly reduced for weakly absorbing but large-sized and irregularly shaped mineral dust particles.

**Table 9. Linear regression parameters including the slope (M), standard deviation of the slope (Std m), intercept (B), standard deviation of intercept (std b), and linear regression coefficient ($R^2$) for the comparison of the CAPS $PM_{ssa}$ and the PSAP instruments.**

| Aerosol | Reference Instrument | m | Std m | b | Std b | $R^2$ |
|---|---|---|---|---|---|---|
| AD | PSAP | 0.89 | 0.01 | 0.00 | 0.00 | 1.00 |
| BC | PSAP | 0.90 | 0.00 | 0.00 | 0.00 | 0.99 |
| MIX | PSAP | 1.02 | 0.04 | 2.02 | 1.16 | 0.99 |
| ALL | PSAP | 0.91 | 0.02 | 0.00 | 0.00 | 0.98 |
| ALL ($\sigma_{ap}$ < 70 $Mm^{-1}$) | PSAP | 1.00 | 0.07 | -3.64 | 2.33 | 0.97 |

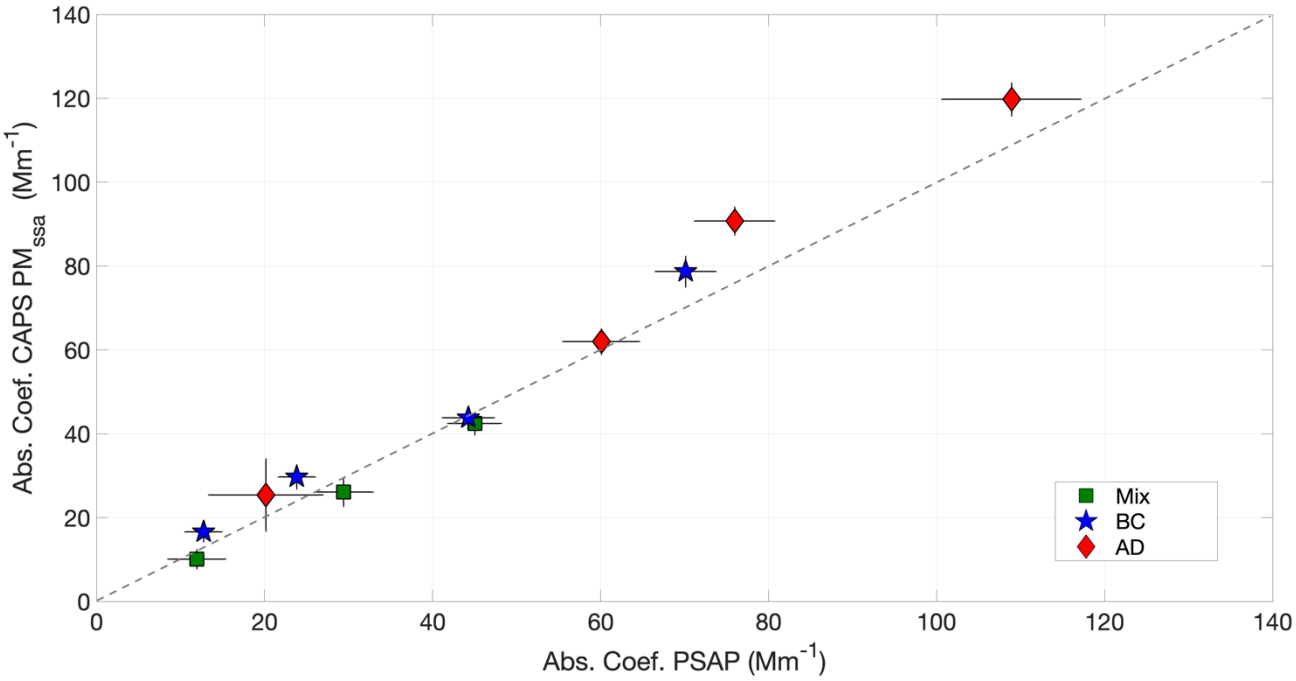


**Figure 13. Comparison result of the absorption indirect measurement by the CAPS $PM_{ssa}$ with the measurements from the PSAP for AD, BC and Mixture (dashed line is the identity line (i.e., 1:1 line)).**

## 3.4 Single Scattering Albedo Measurement

The ultimate property targeted by the CAPS $PM_{ssa}$ is the aerosol single-scattering albedo. Figure 14 shows the average and standard deviation of the SSA measured by the CAPS $PM_{ssa}$ and the applied proven technologies for each aerosol type containing a light-absorbing fraction, at the different extinction coefficient levels. The values for each level are also compiled in Supplemental Table A4.

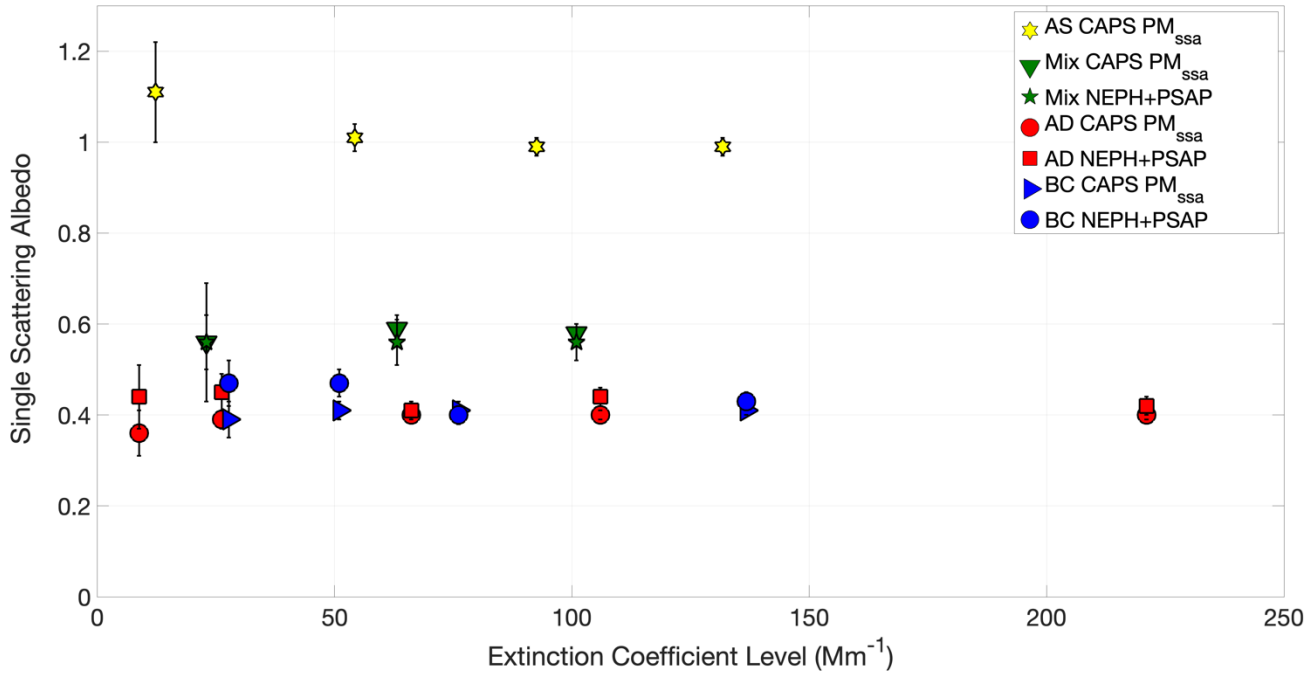


**Figure 14. Average and standard deviation of the measured Single Scattering Albedo as a function of extinction coefficient level for the different aerosols and technologies.**

For the absorbing aerosols, we found maximum deviations between the different SSA values of 0.09, or 18%, with the deviations being randomly distributed around zero. For a single aerosol type, the SSA provided by the CAPS $PM_{ssa}$ shows less scatter around the average value compared to the values derived from PSAP and NEPH data. The measurements by the CAPS $PM_{ssa}$ are more robust in terms of stability in comparison with the values measured by the PSAP+NEPH combination, with an average of the standard deviation for the different aerosol types of 0.01 for the CAPS $PM_{ssa}$ and 0.02 for the PSAP-NEPH combination. It is worth noting that even though there are differences found in the measurements, all measured SSA values fall within the range of values expected for each aerosol type (as measured and detailed in section 3.2 - Table 8).

## 4 Summary and Outlook

An optical closure study has been performed using different types of aerosols (pure scattering, strongly absorbing, and mixture) to evaluate the performance and accuracy of the recently launched Cavity Attenuated Phase-Shift Single Scattering Albedo Monitor.

The results from the instrument intercomparison with proven technologies (CAPS $PM_{ex}$, NEPH, and PSAP) show a very good agreement for all aerosol types, with accuracy of 96% and 99% for the extinction coefficient and scattering coefficient channels, respectively, for all aerosol types. The small deviation of 4% observed in the extinction channel between the CAPS $PM_{ssa}$ and PSAP-NEPH combination originates from the applied correction algorithm to the PSAP data, since it is a logarithmic function of the filter transmission leading to deviations in the dataset. For the evaluation of the performance for each aerosol individually, the extinction channel shows accuracy between 94% and 98%; and the scattering channel, between 94% and 98%. These values are very similar to those found by Petzold et al. (2013) for the CAPS $PM_{ex}$.

Regarding the application of the CAPS $PM_{ssa}$ for the measurement of the absorption coefficient and single-scattering albedo, the instrument has shown good performance on both sides. The accuracy of the absorption coefficient measurement by the CAPS $PM_{ssa}$ in comparison with the PSAP was 91%, as obtained for the linear regression analysis for all investigated aerosol types and aerosol loadings. The large difference observed here comes from the correction scheme applied to the PSAP data at high loadings, as stated earlier. It is possible to observe that the higher deviations occur at high absorption coefficient, also where the transmission of the filter has a steeper decrease. Once the linear regression analysis excludes the points where the average absorption coefficient was higher than 70 $Mm^{-1}$, the slope approaches 100% agreement between the two technologies. For the measurement of SSA, the CAPS $PM_{ssa}$ showed a very good stability for all measured $\sigma_{ep}$ levels, better than the PSAP-NEPH combination. The measured values are within what is expected for the different types of aerosols (0.4 for strongly absorbing aerosols and 1.0 for purely scattering aerosols).

The results reported from our study demonstrate that the CAPS $PM_{ssa}$ is a very robust and reliable instrument for the direct measurement of the scattering and extinction coefficient, as well as for the indirect measurement of the absorption coefficient and single scattering albedo.

## 5 Author Contributions

JP, UB, and AP designed the study and prepared the manuscript, with contributions from all co-authors. AF and TO provided technical details of the instrumentation and contributed to the interpretation of the study results.

## 6 Competing Interests

The authors declare that they have no conflict of interest.

## 7 Acknowledgements

Parts of this work was funded by the EU FP7 project IGAS (Grant Agreement No. 312311), the Federal Ministry of Education and Research, Germany, in IAGOS D (Grant Agreement No. 01LK1301A), EU H2020 Project ENVRIplus (Grant No. 654182) and HITEC Graduate School for Energy and Climate.

## 8 References

Anderson, T. L., Covert, D. S., Marshall, S. F., Laucks, M. L., Charlson, R. J., Waggoner, A. P., Ogren, J. A., Caldow, R., Holm, R. L., Quant, F. R., Sem, G. J., Wiedensohler, A., Ahlquist, N. A., and Bates, T. S.: Performance characteristics of a high-sensitivity, three-wavelength, total scatter/backscatter nephelometer, J. Atmos. Ocean. Technol., 13, 967-986, 10.1175/1520-0426(1996)013<0967:pcoahs>2.0.co;2, 1996.

Andrews, E., Ogren, J. A., Bonasoni, P., Marinoni, A., Cuevas, E., Rodriguez, S., Sun, J. Y., Jaffe, D. A., Fischer, E. V., Baltensperger, U., Weingartner, E., Coen, M. C., Sharma, S., Macdonald, A. M., Leaitch, W. R., Lin, N. H., Laj, P., Arsov, T., Kalapov, I., Jefferson, A., and Sheridan, P.: Climatology of aerosol radiative properties in the free troposphere, Atmos Res, 102, 365-393, 10.1016/j.atmosres.2011.08.017, 2011.

Arnott, W. P., Walker, J. W., Moosmuller, H., Elleman, R. A., Jonsson, H. H., Buzorius, G., Conant, W. C., Flagan, R. C., and Seinfeld, J. H.: Photoacoustic insight for aerosol light absorption aloft from meteorological aircraft and comparison with particle soot absorption photometer measurements: DOE

Southern Great Plains climate research facility and the coastal stratocumulus imposed perturbation experiments, J Geophys Res-Atmos, 111, Artn D05s02
10.1029/2005jd005964, 2006.
Bond, T. C., Anderson, T. L., and Campbell, D.: Calibration and intercomparison of filter-based measurements of visible light absorption by aerosols, Aerosol Sci Tech, 30, 582-600, 1999.
Boucher, O., Randall, D., Artaxo, P., Bretherton, C., Feingold, G., Forster, P., Kerminen, V.-M., Kondo, Y., Liao, H., Lohmann, U., Rasch, P., Satheesh, S. K., Sherwood, S., Stevens, B., and Zhang, X. Y.: Clouds and Aerosols, in: Climate Change 2013: The Physical Science Basis. Contribution of Working Group I to the Fifth Assessment Report of the Intergovernmental Panel on Climate Change, edited by: Stocker, T. F., Qin, D., Plattner, G.-K., Tignor, M., Allen, S. K., Boschung, J., Nauels, A., Xia, Y., Bex, V., and Midgley, P. M., Cambridge University Press, Cambridge, United Kingdom and New York, NY, USA, 571–658, 2013.
Corbin, J. C., Pieber, S. M., Czech, H., Zanatta, M., Jakobi, G., Massabo, D., Orasche, J., El Haddad, I., Mensah, A. A., Stengel, B., Drinovec, L., Mocnik, G., Zimmermann, R., Prevot, A. S. H., and Gysel, M.: Brown and Black Carbon Emitted by a Marine Engine Operated on Heavy Fuel Oil and Distillate Fuels: Optical Properties, Size Distributions, and Emission Factors, J Geophys Res-Atmos, 123, 6175-6195, Artn D027818
10.1029/2017jd027818, 2018.
Han, T. T., Xu, W. Q., Li, J., Freedman, A., Zhao, J., Wang, Q. Q., Chen, C., Zhang, Y. J., Wang, Z. F., Fu, P. Q., Liu, X. G., and Sun, Y. L.: Aerosol optical properties measurements by a CAPS single scattering albedo monitor: Comparisons between summer and winter in Beijing, China, J Geophys Res-Atmos, 122, 2513-2526, 10.1002/2016jd025762, 2017.
Haywood, J. M., and Shine, K. P.: The effect of anthropogenic sulfate and soot aerosol on the clear-sky planetary radiation budget, Geophysical Research Letters, 22, 603-606, 10.1029/95gl00075, 1995.
Heintzenberg, J., and Charlson, R. J.: Design and applications of the integrating nephelometer: A review, J. Atmos. Ocean. Technol., 13, 987-1000, 10.1175/1520-0426(1996)013<0987:daaoti>2.0.co;2, 1996.
Heintzenberg, J., Wiedensohler, A., Tuch, T. M., Covert, D. S., Sheridan, P., Ogren, J. A., Gras, J., Nessler, R., Kleefeld, C., Kalivitis, N., Aaltonen, V., Wilhelm, R. T., and Havlicek, M.: Intercomparisons and aerosol calibrations of 12 commercial integrating nephelometers of three manufacturers, J. Atmos. Ocean. Technol., 23, 902-914, 10.1175/jtech1892.1, 2006.
Lack, D. A., Lovejoy, E. R., Baynard, T., Pettersson, A., and Ravishankara, A. R.: Aerosol absorption measurement using photoacoustic spectroscopy: Sensitivity, calibration, and uncertainty developments, Aerosol Sci Tech, 40, 697-708, 10.1080/02786820600803917, 2006.
Massoli, P., Murphy, D. M., Lack, D. A., Baynard, T., Brock, C. A., and Lovejoy, E. R.: Uncertainty in Light Scattering Measurements by TSI Nephelometer: Results from Laboratory Studies and Implications for Ambient Measurements, Aerosol Sci Tech, 42, 1064-1074, 10.1080/02786820903156542, 2009.
Massoli, P., Kebabian, P. L., Onasch, T. B., Hills, F. B., and Freedman, A.: Aerosol Light Extinction Measurements by Cavity Attenuated Phase Shift (CAPS) Spectroscopy: Laboratory Validation and Field Deployment of a Compact Aerosol Particle Extinction Monitor, Aerosol Sci Tech, 44, 428-435, 10.1080/02786821003716599, 2010.
Moosmüller, H., Varma, R., and Arnott, W. P.: Cavity ring-down and cavity-enhanced detection techniques for the measurement of aerosol extinction, Aerosol Sci Tech, 39, 30-39, 10.1080/027868290903880, 2005.
Muller, T., Virkkula, A., and Ogren, J. A.: Constrained two-stream algorithm for calculating aerosol light absorption coefficient from the Particle Soot Absorption Photometer, Atmos. Meas. Tech., 7, 4049-4070, 10.5194/amt-7-4049-2014, 2014.
Müller, T., Nowak, A., Wiedensohler, A., Sheridan, P., Laborde, M., Covert, D. S., Marinoni, A., Imre, K., Henzing, B., Roger, J.-C., dos Santos, S. M., Wilhelm, R., Wang, Y.-Q., and de Leeuw, G.:

Angular Illumination and Truncation of Three Different Integrating Nephelometers: Implications for Empirical, Size-Based Corrections, Aerosol Sci Tech, 43, 581-586, 10.1080/02786820902798484, 2009.

Ogren, J. A.: Comment on Calibration and Intercomparison of Filter-Based Measurements of Visible Light Absorption by Aerosolso, Aerosol Sci Tech, 44, 589-591, 10.1080/02786826.2010.482111, 2010.

Ogren, J. A., Wendell, J., Andrews, E., and Sheridan, P. J.: Continuous light absorption photometer for long-term studies, Atmos. Meas. Tech., 10, 4805-4818, 10.5194/amt-10-4805-2017, 2017.

Onasch, T. B., Massoli, P., Kebabian, P. L., Hills, F. B., Bacon, F. W., and Freedman, A.: Single Scattering Albedo Monitor for Airborne Particulates, Aerosol Sci Tech, 49, 267-279, 10.1080/02786826.2015.1022248, 2015.

Perim de Faria, J., Bundke, U., Berg, M., Freedman, A., Onasch, T. B., and Petzold, A.: Airborne and laboratory studies of an IAGOS instrumentation package containing a modified CAPS particle extinction monitor, Aerosol Sci Tech, 1-14, 10.1080/02786826.2017.1355547, 2017.

Petzold, A., and Schönlinner, M.: Multi-angle absorption photometry—a new method for the measurement of aerosol light absorption and atmospheric black carbon, Journal of Aerosol Science, 35, 421-441, 10.1016/j.jaerosci.2003.09.005, 2004.

Petzold, A., Onasch, T., Kebabian, P., and Freedman, A.: Intercomparison of a Cavity Attenuated Phase Shift-based extinction monitor (CAPS PMex) with an integrating nephelometer and a filter-based absorption monitor, Atmos. Meas. Tech., 6, 1141-1151, 10.5194/amt-6-1141-2013, 2013.

Sheridan, P. J., Andrews, E., Ogren, J. A., Tackett, J. L., and Winker, D. M.: Vertical profiles of aerosol optical properties over central Illinois and comparison with surface and satellite measurements, Atmospheric Chemistry and Physics, 12, 11695-11721, 10.5194/acp-12-11695-2012, 2012.

Virkkula, A.: Correction of the Calibration of the 3-wavelength Particle Soot Absorption Photometer (3 PSAP), Aerosol Sci Tech, 44, 706-712, 10.1080/02786826.2010.482110, 2010.

## 9 Appendix A

SUPPLEMENTAL INFORMATION

**Table A1.** Extinction coefficient mean and 1-σ standard deviation of the mean measured by the CAPS $PM_{ssa}$ extinction channel and proven technologies

| | | | Run 1 | Run 2 | Run 3 | Run 4 | Run 5 |
|---|---|---|---|---|---|---|---|
| AS | CAPS $PM_{ssa}$ | Av | 54.62 | 127.43 | 311.65 | 198.31 | NA |
| | | Std | 0.29 | 0.66 | 1.04 | 1.50 | NA |
| | CAPS $PM_{ex}$ | Av | 53.39 | 124.78 | 306.40 | 195.94 | NA |
| | | Std | 0.21 | 0.41 | 0.68 | 1.01 | NA |
| AD | CAPS $PM_{ssa}$ | Av | 221.04 | 105.98 | 66.16 | 26.25 | 8.84 |
| | | Std | 1.34 | 0.23 | 0.22 | 0.20 | 0.08 |
| | CAPS $PM_{ex}$ | Av | 210.15 | 100.22 | 63.08 | 24.93 | 8.66 |
| | | Std | 1.53 | 0.22 | 0.16 | 0.14 | 0.05 |
| AD | CAPS $PM_{ssa}$ | Av | 198.00 | 150.09 | 104.15 | 56.88 | 28.85 |
| | | Std | 0.20 | 0.17 | 0.39 | 0.53 | 0.37 |
| | PSAP+NEPH | Av | 187.37 | 135.55 | 102.30 | 51.34 | 26.78 |
| | | Std | 0.33 | 0.23 | 0.36 | 0.61 | 0.34 |
| BC | CAPS $PM_{ssa}$ | Av | 136.77 | 76.16 | 50.99 | 27.73 | NA |
| | | Std | 0.26 | 0.20 | 0.22 | 0.13 | NA |
| | PSAP+NEPH | Av | 134.98 | 81.59 | 48.51 | 26.28 | NA |
| | | Std | 0.22 | 0.18 | 0.16 | 0.29 | NA |
| Mix | CAPS $PM_{ssa}$ | Av | 23.05 | 63.14 | 100.94 | NA | NA |
| | | Std | 0.17 | 0.25 | 0.20 | NA | NA |
| | PSAP+NEPH | Av | 21.28 | 58.47 | 90.83 | NA | NA |
| | | Std | 0.19 | 0.23 | 0.18 | NA | NA |

**Table A2.** Scattering coefficient mean and 1-σ standard deviation of the mean measured by the CAPS $PM_{ssa}$ and NEPH

| | | | Run 1 | Run 2 | Run 3 | Run 4 | Run 5 |
|---|---|---|---|---|---|---|---|
| AS | CAPS $PM_{ssa}$ | Av | 131.79 | 92.57 | 54.29 | 12.31 | NA |
| | | Std | 0.11 | 0.16 | 0.08 | 0.06 | NA |
| | NEPH | Av | 133.22 | 93.22 | 54.18 | 11.77 | NA |
| | | Std | 0.11 | 0.10 | 0.08 | 0.04 | NA |
| AD | CAPS $PM_{ssa}$ | Av | 78.29 | 59.42 | 41.18 | 21.98 | 10.32 |
| | | Std | 0.11 | 0.10 | 0.16 | 0.22 | 0.15 |
| | NEPH | Av | 78.50 | 59.86 | 41.70 | 22.93 | 11.87 |
| | | Std | 0.12 | 0.12 | 0.17 | 0.22 | 0.17 |
| BC | CAPS $PM_{ssa}$ | Av | 54.33 | 30.54 | 20.58 | 10.66 | NA |
| | | Std | 0.14 | 0.11 | 0.11 | 0.08 | NA |
| | NEPH | Av | 52.71 | 29.81 | 20.91 | 11.31 | NA |
| | | Std | 0.14 | 0.11 | 0.12 | 0.08 | NA |
| Mix | CAPS $PM_{ssa}$ | Av | 11.66 | 32.52 | 51.09 | NA | NA |
| | | Std | 0.11 | 0.14 | 0.14 | NA | NA |
| | NEPH | Av | 11.32 | 34.05 | 54.43 | NA | NA |
| | | Std | 0.11 | 0.14 | 0.12 | NA | NA |

**Table A3.** Absorption coefficient mean and 1-σ standard deviation of the mean measured by the CAPS $PM_{ssa}$ (extinction minus scattering) and PSAP

| | | | Run 1 | Run 2 | Run 3 | Run 4 | Run 5 |
|---|---|---|---|---|---|---|---|
| BC | CAPS $PM_{ssa}$ | Av | 78.69 | 43.78 | 29.73 | 16.57 | NA |
| | | Std | 0.18 | 0.13 | 0.14 | 0.09 | NA |
| | PSAP | Av | 70.13 | 44.27 | 23.85 | 12.74 | NA |
| | | Std | 0.19 | 0.16 | 0.12 | 0.09 | NA |
| AD | CAPS $PM_{ssa}$ | Av | 119.75 | 90.76 | 62.02 | 25.40 | 18.53 |
| | | Std | 0.14 | 0.13 | 0.24 | 0.32 | 0.23 |
| | PSAP | Av | 108.92 | 75.97 | 60.09 | 20.16 | 14.92 |
| | | Std | 0.31 | 0.19 | 0.23 | 0.40 | 0.20 |
| Mix | CAPS $PM_{ssa}$ | Av | 10.09 | 26.09 | 42.44 | NA | NA |
| | | Std | 0.10 | 0.16 | 0.11 | NA | NA |
| | PSAP | Av | 11.95 | 29.42 | 45.03 | NA | NA |
| | | Std | 0.18 | 0.17 | 0.14 | NA | NA |

**Table A4.** Single Scattering Albedo average value and standard deviation for CAPS $PM_{ssa}$ and proven technologies

| | Scat/Ext | | Run 1 | Run 2 | Run 3 | Run 4 | Run 5 |
|---|---|---|---|---|---|---|---|
| AS | CAPS $PM_{ssa}$ | Av | 0.99 | 0.99 | 1.01 | 1.09 | NA |
| | | Std | 0.02 | 0.02 | 0.03 | 0.11 | NA |
| AD | CAPS $PM_{ssa}$ | Av | 0.40 | 0.40 | 0.40 | 0.39 | 0.36 |
| | | Std | 0.01 | 0.01 | 0.01 | 0.02 | 0.05 |
| | PSAP+NEPH | Av | 0.42 | 0.44 | 0.41 | 0.45 | 0.44 |
| | | Std | 0.02 | 0.02 | 0.02 | 0.04 | 0.07 |
| BC | CAPS $PM_{ssa}$ | Av | 0.40 | 0.40 | 0.40 | 0.38 | NA |
| | | Std | 0.01 | 0.02 | 0.02 | 0.04 | NA |
| | PSAP+NEPH | Av | 0.39 | 0.37 | 0.43 | 0.43 | NA |
| | | Std | 0.02 | 0.02 | 0.03 | 0.05 | NA |
| Mix | CAPS $PM_{ssa}$ | Av | 0.51 | 0.52 | 0.51 | NA | NA |
| | | Std | 0.06 | 0.03 | 0.02 | NA | NA |
| | PSAP+NEPH | Av | 0.53 | 0.58 | 0.60 | NA | NA |
| | | Std | 0.13 | 0.05 | 0.04 | NA | NA |